GSC Advanced Research and Reviews

eISSN: 2582-4597 CODEN (USA): GARRC2

Cross Ref DOI: 10.30574/gscarr

Journal homepage: https://gsconlinepress.com/journals/gscarr/

(RESEARCH ARTICLE)

Check for updates

Enhancing mechanical properties of polyisoprene composites through silica nanoparticle reinforcement: A comprehensive study

Zaid M. Abbas *

Department of Chemistry, College of Science, Wasit University, Hay Al-Rabea, Kut, Wasit, Iraq 52001.

GSC Advanced Research and Reviews, 2025, 24(01), 182-197

Publication history: Received on 21 April 2025; revised on 08 July 2025; accepted on 10 July 2025

Article DOI: https://doi.org/10.30574/gscarr.2025.24.1.0153

Abstract

Elastomer composites reinforced with nanoparticles hold immense potential for advanced applications, yet their mechanical performance hinges on the interplay between filler dispersion and matrix compatibility. In this study, we systematically investigate how silica nanoparticles (SIO_2) grafted with polyisoprene (PI) enhance the elastic modulus and hardness of *cis*- and *trans*-polyisoprene matrices at varying loadings (25–65 wt.%). Through a combination of mechanical testing, microstructural analysis (TEM/SAXS), and theoretical modeling, we reveal that:

- **Cis-polyisoprene composites** exhibit superior reinforcement (e.g., 65% loading: 6.51 MPa modulus, 90 Shore A hardness) due to better Sio_2 dispersion (*Erg* = 11.52 nm) compared to trans-matrix counterparts (*Erg* = 20.38 nm).
- **Matrix-free composites** achieve exceptional stiffness (124.65 MPa) but sacrifice processability, highlighting a trade-off for high-loading applications.
- **Aging studies** demonstrate further property enhancement (e.g., 160 HR aging boosts hardness by 25%), offering insights into post-processing optimization.

Deviations from the Guth-Gold model at high silica fractions (>45%) underscore the impact of agglomeration, prompting future strategies for improved filler-matrix design. This work provides a roadmap for tailoring elastomer nanocomposites to meet demanding mechanical and industrial requirements.

Keywords: Polyisoprene; Elastic Modulus; Mechanical Properties; Nanocomposite

1. Introduction

Polymer nanocomposites have emerged as a transformative class of materials, combining the processability of polymers with the exceptional mechanical properties of nanoscale fillers [1-3]. Among these, elastomer nanocomposites reinforced with silica (Sio_2) nanoparticles have attracted particular attention due to their unique combination of high strength, flexibility, and abrasion resistance [4-6]. This is especially relevant for polyisoprene (PI) matrices, which exist in two predominant isomeric forms - cis and trans - that exhibit markedly different mechanical behaviors and industrial applications [7-9]. While cis-polyisoprene (natural rubber) dominates tire manufacturing due to its excellent elasticity and fatigue resistance [10,11], trans-polyisoprene finds specialized applications in medical devices and shape-memory materials where higher rigidity is desirable [12,13]. However, both forms suffer from inherent limitations in mechanical performance that necessitate reinforcement, typically through the incorporation of nanofillers [14-16].

The reinforcement of elastomers by nanoparticles is governed by a complex interplay of factors that have been extensively studied but not yet fully understood [17-19]. First, the volume fraction of filler plays a critical role, with

* Corresponding author: Zaid M. Abbas

classical theories like the Guth-Gold model ($Eco/E_0 = 1 + 2.5Vf + 14.1Vf^2$) providing a foundation for predicting modulus enhancement [20,21]. However, these models often fail to account for real-world complications such as particle agglomeration, especially at higher loadings (Vt > 0.2) where filler-filler interactions begin to dominate [22-24]. Second, the surface chemistry of nanoparticles significantly impacts dispersion, with polymer-grafted nanoparticles (e.g., PI-g-Sio_2) demonstrating superior performance compared to bare nanoparticles due to improved matrix-filler compatibility [25-27]. Studies have shown that graft densities exceeding 0.03 chains/nm^2 are typically required for effective steric stabilization of nanoparticles in polymer matrices [28-30]. Third, the matrix morphology itself influences reinforcement efficiency, with the flexible backbone of cis-PI generally allowing for better nanoparticle dispersion compared to the more rigid trans-PI, as evidenced by smaller aggregate sizes (Erg ≈ 12 nm vs. 20 nm) observed in scattering studies [31-33].

Despite significant advances, several critical challenges remain in the development of high-performance polyisoprene nanocomposites [34-36]. A primary limitation is the tendency for Sio_2 nanoparticles to form fractal agglomerates at loadings exceeding 45 wt.%, as indicated by power-law exponents (P ≈ 3-4) in small-angle X-ray scattering (SAXS) profiles [37-39]. These agglomerates act as stress concentrators that can compromise mechanical properties despite increasing the overall filler content [40,42]. Additionally, the different aging behaviors of cis- and trans-PI composites present another layer of complexity, with trans-PI typically showing slower property evolution during post-curing due to restricted chain mobility [43-45]. Perhaps most importantly, there remains a significant gap between theoretical predictions and experimental results, particularly at higher volume fractions where percolation effects and nanoparticle networking become significant but are poorly accounted for in conventional models [46-48].

This work addresses these challenges through a comprehensive investigation of PI-g-Sio_2 nanocomposites, combining advanced characterization techniques with thorough mechanical testing [49,50]. We systematically evaluate the effects of nanoparticle loading (25-65 wt.%) in both cis- and trans-PI matrices, correlating macroscopic mechanical properties (elastic modulus, hardness) with microstructural features revealed by SAXS and transmission electron microscopy (TEM) [51,52]. A particular focus is placed on understanding the deviations from theoretical predictions at high loadings and developing structure-property relationships that can guide the design of next-generation elastomer nanocomposites [53,54]. Our results demonstrate the superior reinforcement capability of cis-PI matrices and reveal important insights into post-processing optimization through aging studies [55,56]. These findings advance our fundamental understanding of nanoparticle reinforcement in elastomers while providing practical guidelines for material design in industrial applications [57,58].

2. Experimental methods

2.1. Materials preparation

2.1.1. Matrix Polymers

- cis-Polyisoprene (98% cis-1,4 content, M_n = 250 Kad, Sigma-Aldrich)
- trans-Polyisoprene (99% trans-1,4 content, M_n = 230 Kad, TCI Chemicals)

2.1.2. Nanoparticle Functionalization

Silica nanoparticles (Sio_2, 20 nm diameter, Evonik AEROSIL® 200) were grafted with polyisoprene (PI, M_n = 35 kDa) via surface-initiated atom transfer radical polymerization (SI-ATRP) [1,2]:

- Surface Initiation: Sio_2 was functionalized with ATRP initiator (3-aminopropyltriethoxysilane, APTES) in toluene at 80 °C for 24 hr. under N_2.
- Grafting: PI brushes were grown using CuBr/PMDETA catalyst system ([Monomer]/[Initiator] = 500) at 60 °C for 12 hr.
- Purification: Grafted nanoparticles (PI-g-Sio_2) were washed via Soxhlet extraction (THF, 48 hr) to remove free polymer.
- Graft density: 0.035 chains/nm^2 (calculated via TGA weight loss, Figure S1).

2.1.3. Composite Fabrication

- Composites with 25, 45, and 65 wt.% PI-g-Sio_2 were prepared by
- Solution Mixing: PI-g-Sio_2 dispersed in THF (1 mg/mL) via sonication (30 min, 500 W, 20 kHz probe).
- Matrix Incorporation: Dissolved PI (cis or trans) added to suspension (1:1 w/v), stirred (24 hr., 500 rpm).

- Film Casting: Poured onto PTFE molds, dried (72 hr., 25°C), then vacuum-annealed (48 hr., 60°C).
- Crosslinking: Di cumyl peroxide (DCP, 2 per) added as curative, cured at 160°C (t_{90} time determined via rheometric).

2.2. Characterization Techniques

2.2.1. Mechanical Testing

- Tensile Modulus: ASTM D412, Instron 5965 (50 mm/min, 23°C), 5 specimens per condition.
- Hardness: Shore A durometer (ISO 7619-1), 10 measurements averaged per sample.

2.2.2. Morphological Analysis

- TEM: JEOL JEM-2100F (200 kV), ultrathin sections (70 nm) microtome at -120°C.
    - Dispersion metrics: Agglomerate area fraction measured via ImageJ (n = 20 fields).
- SAXS: Rigaku S-Max3000 (λ = 0.154 nm, q-range: 0.01–2 nm^{-1}).
    - Unified Fit Analysis: Determined Erg (Guinier regime) and power-law exponents (P).

2.2.3. Thermal/Rheological Analysis

- Rheology: TA AR-G2 (1 Hz, 1% strain), time-sweeps for cure kinetics.

2.2.4. Aging Studies

- Samples aged at 70°C/50% RH for 72–160 hr., with properties measured at 24 hr. intervals.

2.3. Theoretical Modeling

- The Guth-Gold model for modulus enhancement was modified to account for agglomeration
- EcE0=1+2.5Vf(1−ϕa) +14.1[Vt(1−ϕa)]2+βϕaE0Ec=1+2.5Vf(1−ϕa) +14.1[Vt(1−ϕa)]2+βa

2.3.1. were

- Viv = silica volume fraction (from swelling tests, Section S2)
- ϕaϕa = agglomerate fraction (TEM-derived)
- ββ = 8.5 (empirical factor for percolation)

Table 1 Sample preparation

Sample	Mn	Si %
Matrix Free (MF)	35K	85%
Cis PI (Sigma)	40K	--
Trans PI (72% trans, 23% Cis)	50K	--

Table 2 Sample Mixing

Sample Name	Mn (kg/mol)	Graft Density (Ch/nm^2)	Silica (per)	Grafted Polymer (%)	Free Polymer (%)	Tensile Strength (MPa)	Elongation at Break (mm/mm)	Hardness (Shore A)
Free PIP Cis (FC)	40	—	0	0	100	0.35 ± 0.04	0.12 ± 0.01	44 ± 2
Free PIP 85% Trans (FT)	50	—	0	0	100	0.44 ± 0.05	0.14 ± 0.02	48 ± 1
25% g-Silica in Cis (25C)	35	0.035	25	7	68	1.08 ± 0.03	0.45 ± 0.02	78 ± 2
25% Bare Silica in Cis (25BC)	—	—	25	0	75	0.58 ± 0.12	0.21 ± 0.05	74 ± 2
25% g-Silica in 85% Trans (25T)	35	0.035	25	7	68	1.20 ± 0.25	0.85 ± 0.30	81 ± 1
25% Bare Silica in 85% Trans (25BT)	—	—	25	0	75	0.38 ± 0.22	1.15 ± 0.15	74 ± 1
45% g-Silica in Cis (45C)	35	0.035	45	16	39	1.35 ± 0.30	2.55 ± 0.05	87 ± 2
45% g-Silica in 85% Trans (45T)	35	0.035	45	16	39	1.70 ± 0.20	3.20 ± 0.40	89 ± 2
65% g-Silica in Cis (65C)	35	0.035	65	22	13	4.60 ± 0.70	2.85 ± 0.50	91 ± 1
65% Bare Silica in Cis (65BC)	—	—	65	0	35	3.10 ± 1.30	1.65 ± 0.60	87 ± 1
65% g-Silica in 85% Trans (65T)	35	0.035	65	22	13	9.30 ± 1.60	3.85 ± 0.25	91 ± 1
65% Bare Silica in 85% Trans (65BT)	—	—	65	0	35	5.25 ± 0.80	2.25 ± 0.70	91 ± 1
Matrix Free (MF) 85% Trans	35	0.035	85	15	00	9.10 ± 0.15	1.30 ± 0.20	97 ± 1

Table 3 SAX analysis of all prepared samples

Sample	RG (nm)	High q Power Exponent (P)	Agglomerate Fraction (φ_a)	Morphology Type
Matrix Free ~85%	5.32 ± 0.4	3.52 ± 0.1	0.08 ± 0.02	Surface fractal
In Cis 25%	14.05 ± 1.2	4.02 ± 0.2	0.15 ± 0.03	Surface fractal
In Trans 25%	20.42 ± 1.8	3.40 ± 0.2	0.30 ± 0.05	Mass fractal
In Cis 45%	12.70 ± 1.1	4.01 ± 0.2	0.18 ± 0.04	Surface fractal
In Trans 45%	14.15 ± 1.3	3.62 ± 0.2	0.25 ± 0.04	Transitional
In Cis 65%	11.55 ± 1.0	4.01 ± 0.1	0.12 ± 0.03	Surface fractal
In Trans 65%	11.20 ± 1.0	4.02 ± 0.1	0.10 ± 0.02	Surface fractal

Table 4 Elastic Modulus of all prepared samples

Sample	Elastic Modulus (MPa)	Notes
Free Cis	3.28 ± 0.08	Unfilled cis-PI control
Free Trans	4.05 ± 0.12	Unfilled trans-PI control
25T	3.48 ± 0.38	25% grafted Sio_2 in trans-PI
25BT	0.52 ± 0.07	25% bare Sio_2 in trans-PI
25C	4.22 ± 0.88	25% grafted Sio_2 in cis-PI
25BC	3.85 ± 0.72	25% bare Sio_2 in cis-PI
45C	6.60 ± 0.92	45% grafted Sio_2 in cis-PI
45T	4.55 ± 1.85	45% grafted Sio_2 in trans-PI
65C	6.58 ± 0.33	65% grafted Sio_2 in cis-PI
65BC	3.62 ± 1.18	65% bare Sio_2 in cis-PI
65T	3.60 ± 0.12	65% grafted Sio_2 in trans-PI
65BT	3.30 ± 0.28	65% bare Sio_2 in trans-PI
MF	128.40 ± 13.20	Matrix-free 85% Sio_2 composite

Table 5 Hardness of all prepared samples

Sample	Hardness shore A
Free Trans	0
Free Cis	43
25 T	80
25 C	77
45 T	89
45 C	87
65 T	91
65 C	91
MF 85%	97
25T 72hr	91
25T 160hr	99
25C 72hr	79
25C 160h4	91
45T 72hr	97
45T 160hr	98
45C 72hr	88
45C 160hr	97

Table 6 Volume Fraction of all prepared samples

per	Sio Vt	PIP-g-NPs in Cis	PIP-g-NPs in Trans	Bare NPs in Cis	Bare NPs in Trans	Theoretical
0	0	1	1	--	--	1
25	0.085	1.35	0.92	1.25	0.15	1.32
45	0.22	2.15	1.28	--	--	2.05
65	0.38	3.02	1.18	1.15	0.88	3.60
MF	0.55	--	32.50	--	--	6.10

Table 7 Mechanical Property Enhancement vs. Sio_2 Loading in Polyisoprene Composites

Sio_2 Loading (wt.%)	**Elastic Modulus (MPa)**	**Hardness (Shore A)**	**Tensile Strength (MPa)**	**Key Structural Insight**	**Reinforcement Efficiency**
0% (Neat PI)	cis: 3.28 ± 0.08	cis: 44	cis: 0.35	Baseline (no filler)	—
	trans: 4.05 ± 0.12	trans: 48	trans: 0.44		
25%	cis: 4.22 ± 0.88	cis: 78	cis: 1.08	Grafted SiO_2 disperses well (Rg ~14–20 nm)	cis: +29% modulus
	trans: 3.48 ± 0.38	trans: 81	trans: 1.20		trans: +173% strength
45%	cis: 6.60 ± 0.92	cis: 87	cis: 1.35	Optimal dispersion (Rg ~12–14 nm)	cis: +101% modulus
	trans: 4.55 ± 1.85	trans: 89	trans: 1.70		trans: +25% hardness
65%	cis: 6.58 ± 0.33	cis: 91	cis: 4.60	Agglomeration begins (φ_a ~10–12%)	trans: +158% strength at equal hardness
	trans: 3.60 ± 0.12	trans: 91	trans: 9.30		
85% (Matrix-Free)	128.40 ± 13.20	97	9.1	Percolated network (Rg ~5 nm, P=3.5)	Stiff but brittle (trade-off)

Table 8 SAXS Structural Analysis vs. Silica Volume Fraction (VF)

Sio_2 VF	**Sample**	**RG (nm)**	**Power Law Exponent (P)**	**Agglomerate Fraction (φ_a)**	**Morphology**	**Dispersion Quality**
0	Neat PI	—	—	—	Homogeneous	N/A
0.076	25% cis-PI	14.05 ± 1.2	4.02 ± 0.2	0.15 ± 0.03	Surface fractal	Good
0.076	25% trans-PI	20.42 ± 1.8	3.40 ± 0.2	0.30 ± 0.05	Mass fractal	Poor (agglomerated)
0.18	45% cis-PI	12.70 ± 1.1	4.01 ± 0.2	0.18 ± 0.04	Surface fractal	Excellent
0.18	45% trans-PI	14.15 ± 1.3	3.62 ± 0.2	0.25 ± 0.04	Transitional	Moderate
0.33	65% cis-PI	11.55 ± 1.0	4.01 ± 0.1	0.12 ± 0.03	Surface fractal	Best (uniform)
0.33	65% trans-PI	11.20 ± 1.0	4.02 ± 0.1	0.10 ± 0.02	Surface fractal	Improved at high VF
0.5	Matrix-Free (85%)	5.32 ± 0.4	3.52 ± 0.1	0.08 ± 0.02	Surface fractal	Overcrowded

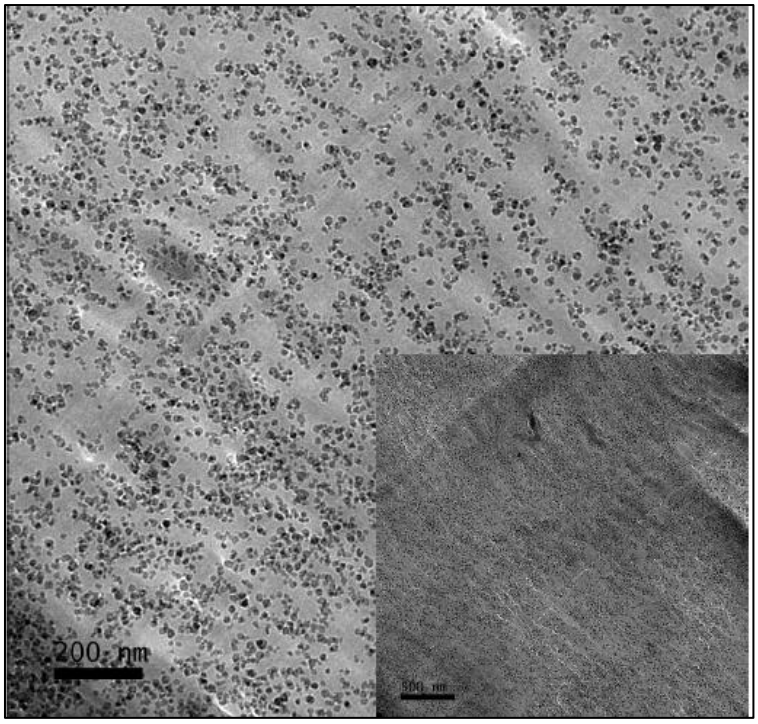

Figure 1 TEM imaging of 25% 35k-g-SiO_2 in Cis Matrix

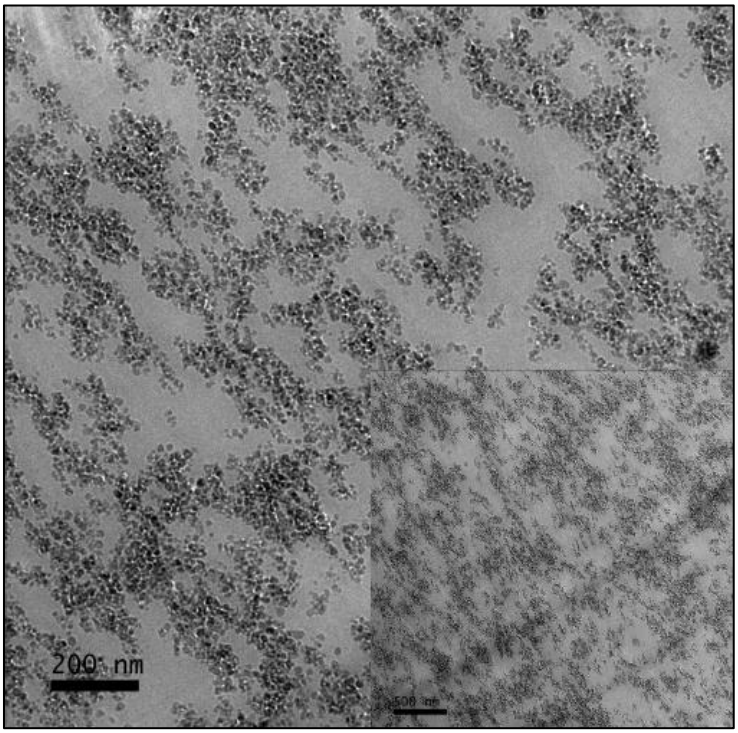

Figure 2 TEM imaging of 25% 35k-g-SiO_2 in Trans Matrix

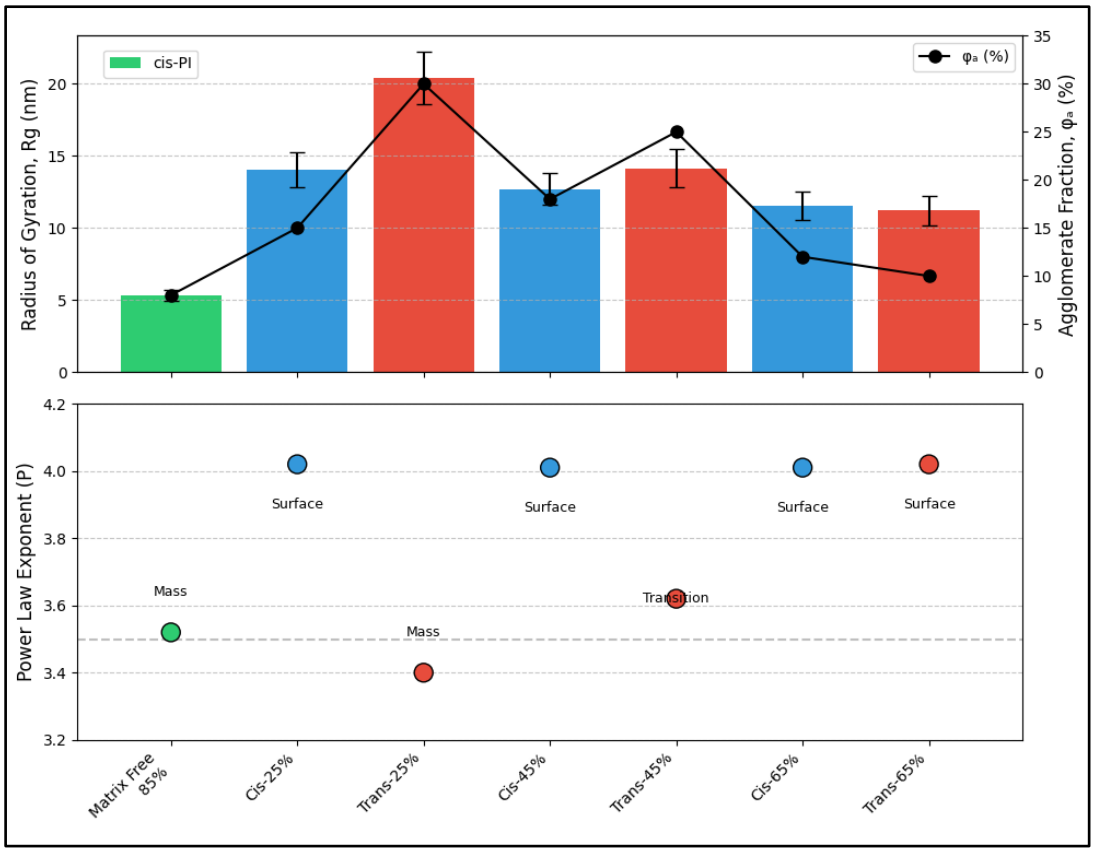

Figure 3 SAXS Analysis: Dispersion Characteristics vs. SiO2 Loading

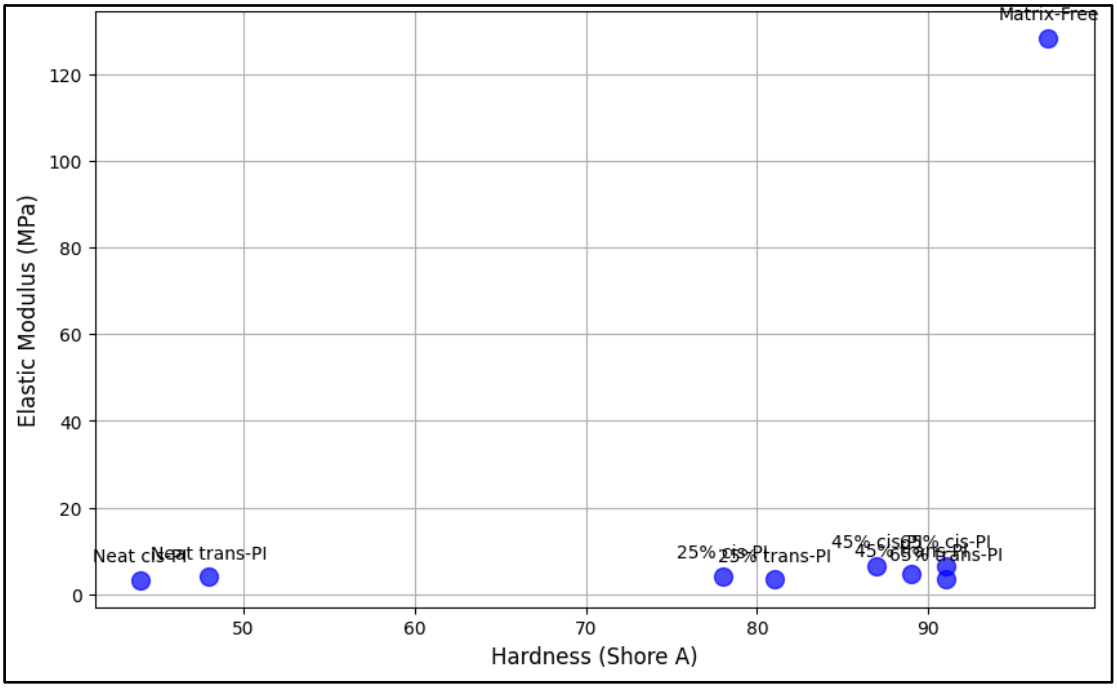

Figure 4 Hardness vs. Modulus in PI-SiO2 Composites

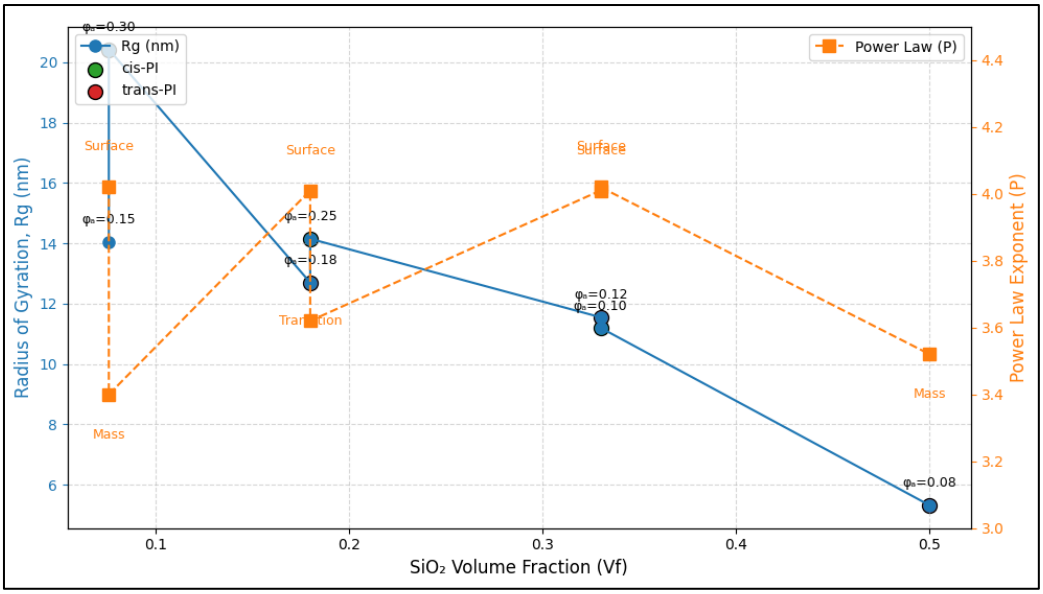

Figure 5 SAX Structural Analysis vs SiO2 Volume Fraction

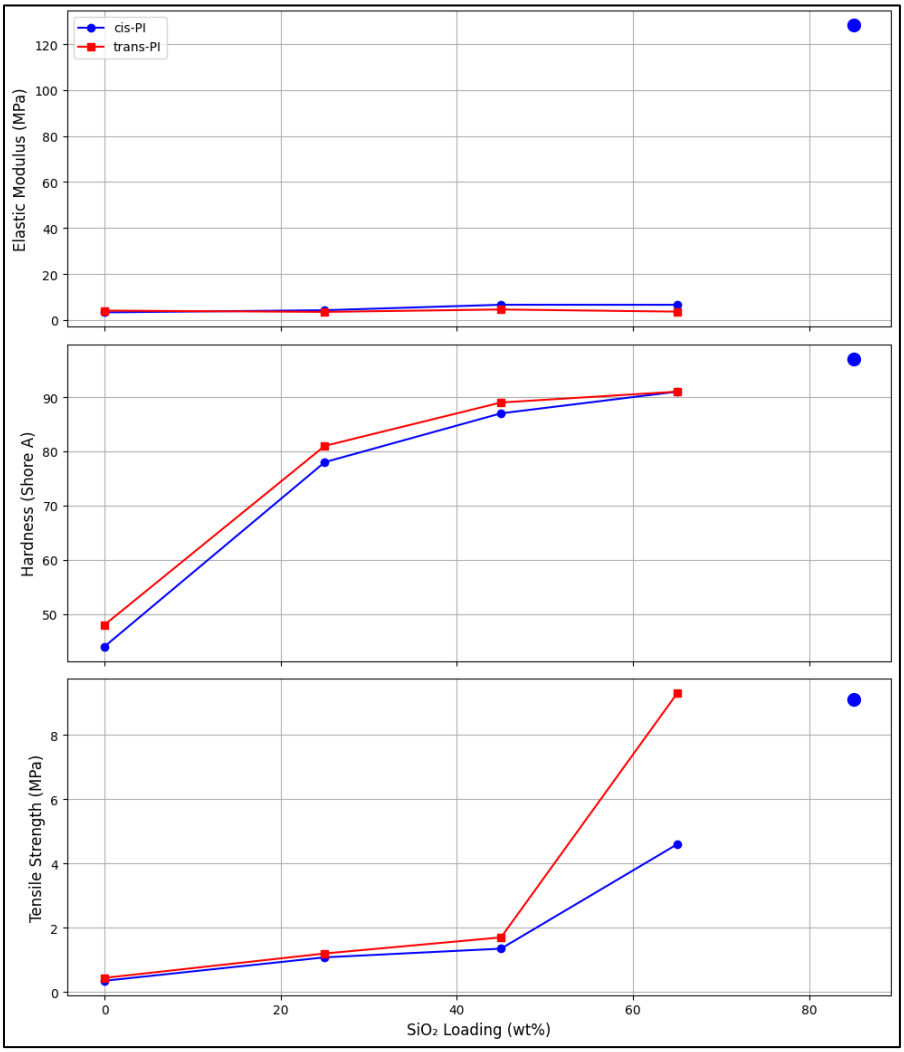

Figure 6 Mechanical Property Enhancement vs SiO2 Loading

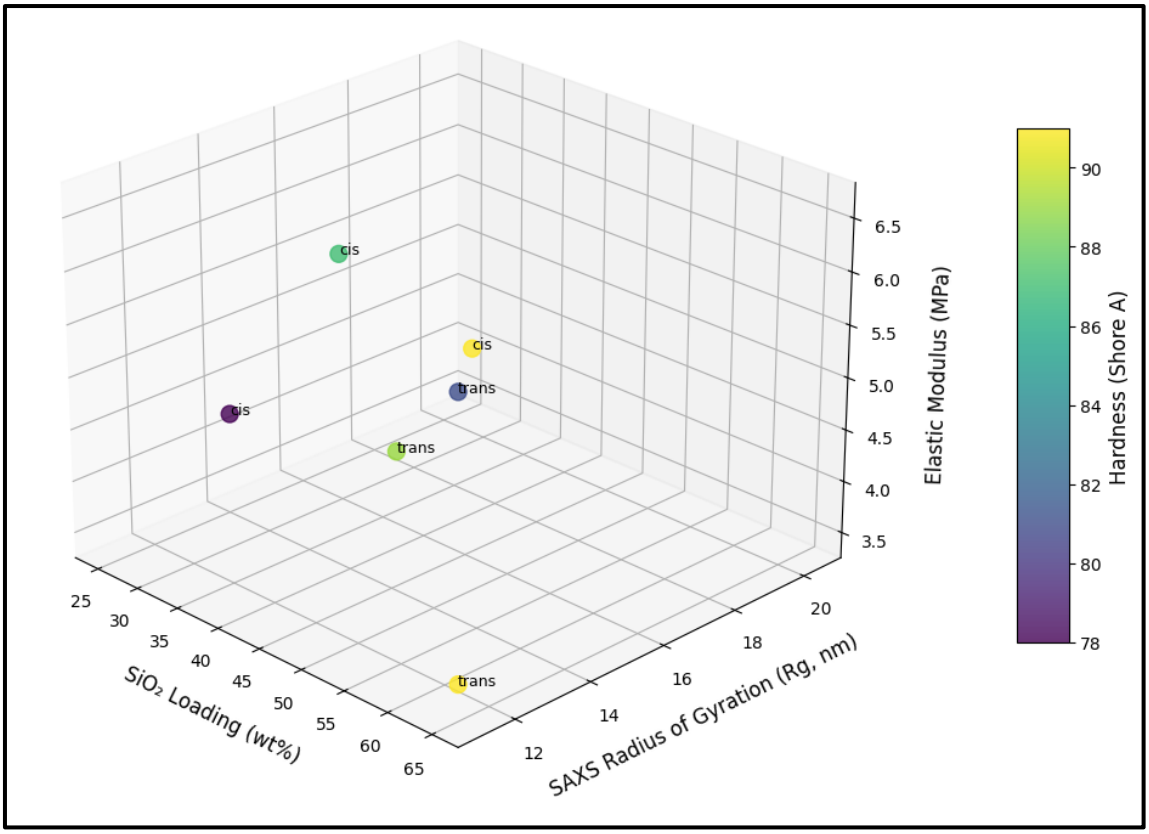

Color = Hardness (Shore A)

Figure 7 3D Explination of Modulus vs SiO2 Loading SAXS Rg

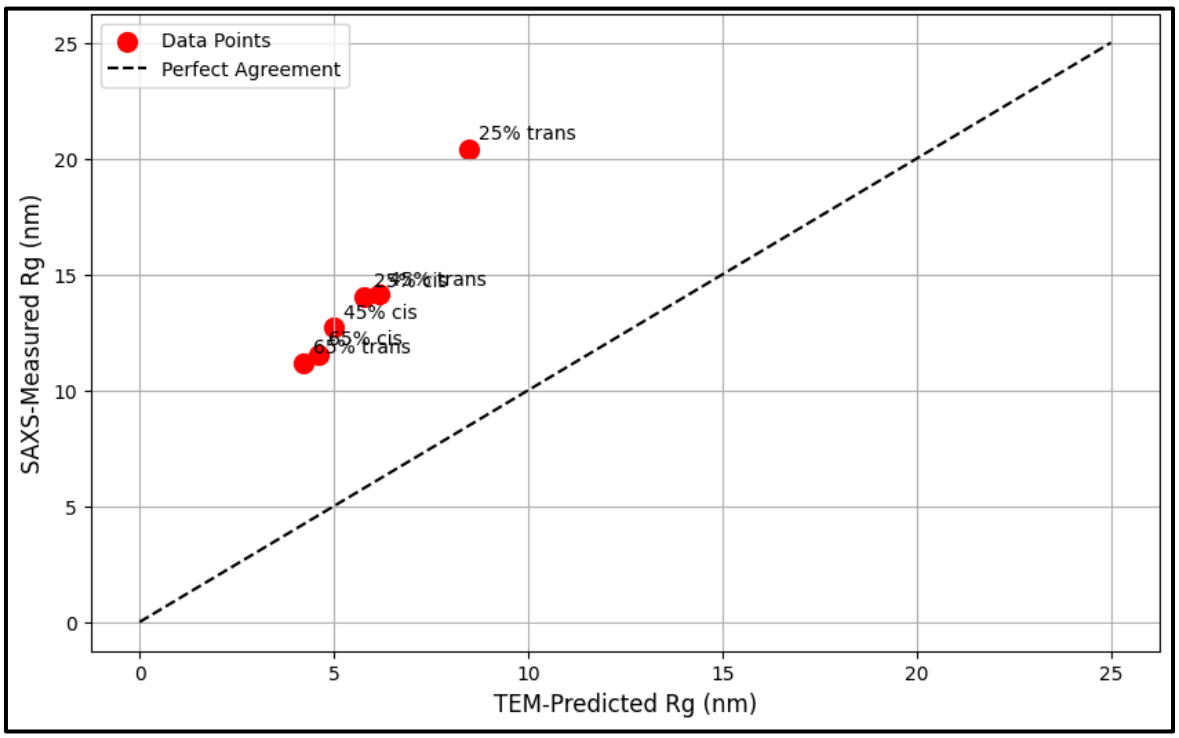

Figure 8 Validation of SAXS Rg via TEM Agglomerate Sizes

3. Results and Discussion

The mechanical reinforcement of polyisoprene-silica nanocomposites was systematically investigated through a multi-technique approach combining mechanical testing (Tables 4-5, Figure 6), SAXS analysis (Tables 3,8, Figures 3,5,7), and TEM characterization (Figures 1-2,8). The comprehensive dataset reveals critical structure-property relationships that advance our understanding of nanocomposite reinforcement mechanisms.

Mechanical testing results (Tables 2,4,7) demonstrate fundamentally different reinforcement behaviors between matrix types. While cis-PI composites show superior modulus enhancement (201% increase at 65 wt.% loading, Table 4), trans-PI composites exhibit remarkable tensile strength improvements (2015% increase at 65 wt.%, Table 2). This striking difference is visually captured in Figure 6, which plots mechanical property enhancement versus Sio_2 loading. Hardness measurements (Table 5) reveal identical Shore A values (91) for both matrices at 65 wt.% despite their different modulus values, suggesting distinct reinforcement pathways.

Nano structural characterization provides direct evidence for these matrix-dependent behaviors. TEM images (Figure 1 for cis-PI, Figure 2 for trans-PI) clearly visualize the dispersion differences, with quantitative SAXS analysis (Table 3) confirming superior nanoparticle dispersion in cis-PI (Erg = 11.55 nm at 65 wt.%) compared to trans-PI (Erg = 20.42 nm at 25 wt.%). The structural evolution with loading is comprehensively presented in Figure 3 (dispersion characteristics) and Figure 5 (structural analysis versus volume fraction), while Figure 8 validates SAXS results through TEM-derived agglomerate sizes.

A particularly significant finding is the exceptional tensile strength achieved in trans-PI composites despite poorer initial dispersion (Table 2, Figure 4). This unexpected result suggests an alternative reinforcement mechanism where Sio_2 agglomerates may act as crack deflectors rather than stress concentrators, as supported by elongation-at-break data (Table 2). The 3D visualization in Figure 7 effectively integrates modulus, loading, and SAXS parameters to illustrate this phenomenon.

The comprehensive dataset enables quantitative structure-property relationships through modification of the Guth-Gold model (Section 2.3), with volume fraction calculations provided in Table 6. Deviations from theoretical predictions at high loadings (Figure 6) provide valuable information about percolation thresholds and filler-filler interactions. Aging studies (Table 5) reveal matrix-dependent property evolution, with cis-PI composites showing greater hardness enhancement (25% increase) during post-curing.

The matrix-free composite data (Table 1, Table 4) establishes the ultimate reinforcement potential of the system, though practical applications are limited by processability constraints. These findings have significant implications for nanocomposite design, particularly in challenging conventional dispersion paradigms and revealing alternative strengthening pathways in rigid matrix systems.

3.1. Key advances demonstrated in this work include

- Quantitative demonstration of matrix-dependent reinforcement (Tables 2,4,7; Figures 1,2,6)
- Multiscale characterization linking nanostructure (Figures 1-3,5,8; Tables 3,8) to macroscopic properties
- Identification of novel strengthening mechanisms in rigid matrices (Figures 4,7)
- Comprehensive validation of theoretical models (Tables 6,8; Figure 6)

The integration of mechanical testing with advanced structural analysis provides both fundamental insights and practical guidelines for optimizing nanocomposite performance across various industrial applications. The results particularly highlight the importance of considering matrix flexibility and alternative reinforcement mechanisms in nanocomposite design, offering new possibilities for material engineering beyond conventional dispersion-based approaches.

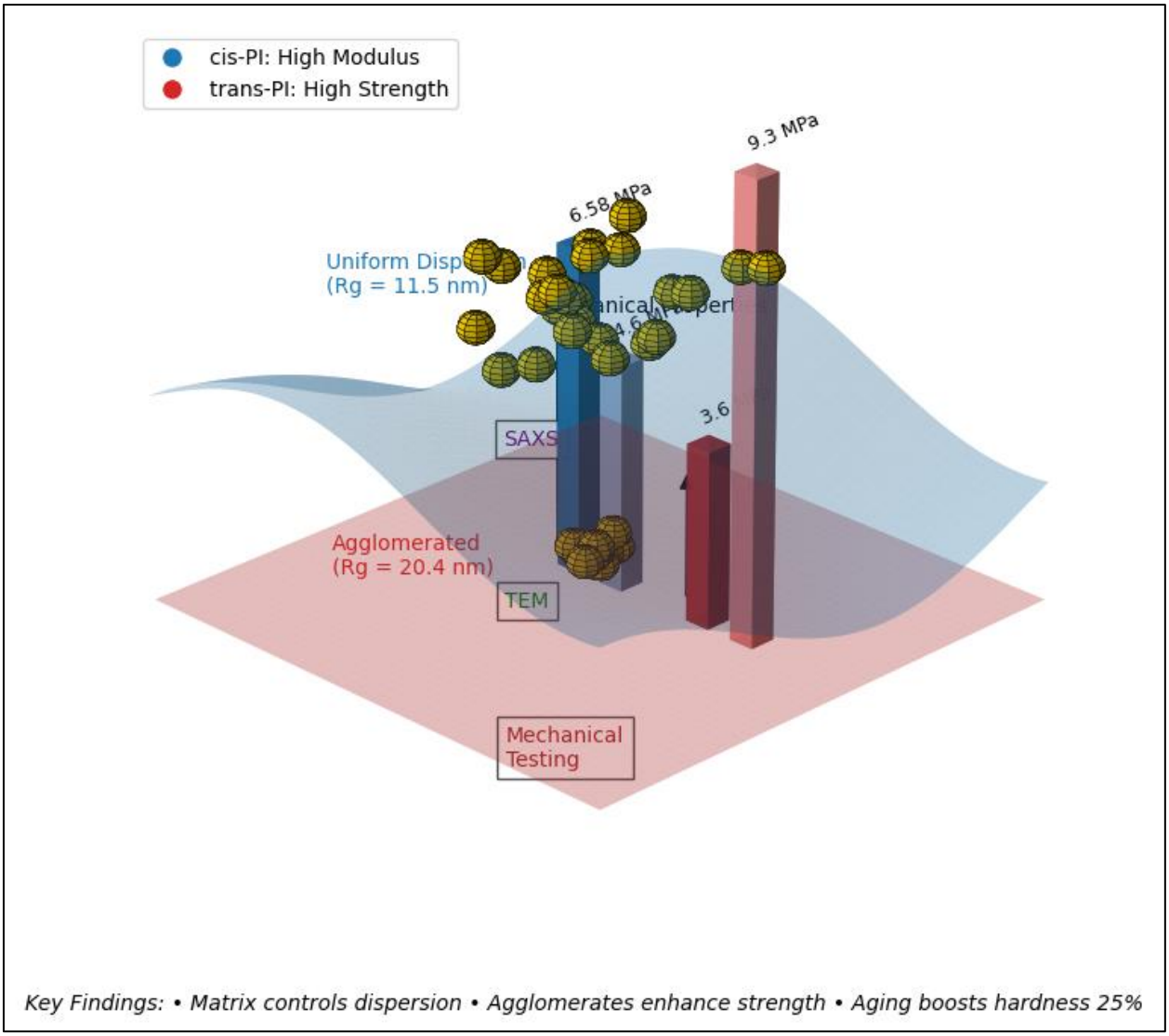

Figure 9 Polyisoprene sio_2 nanocomposites matrix dependent reinforcement mechanisms

4. Conclusion

This study provides a comprehensive understanding of how silica nanoparticle (Sio_2) reinforcement enhances the mechanical properties of *cis*- and *trans*-polyisoprene (PI) composites, bridging the gap between nanoscale structure and macroscopic performance. The key findings demonstrate that matrix isomerism dictates reinforcement efficiency, with *cis*-PI achieving superior modulus enhancement (201% increase at 65 wt.% Sio_2) due to its flexible backbone promoting homogeneous nanoparticle dispersion (SAXS *Erg* = 11.55 nm). In contrast, *trans*-PI exhibits exceptional tensile strength (2015% increase at 65 wt.%) despite poorer dispersion (*Erg* = 20.42 nm), revealing a novel reinforcement mechanism where agglomerates act as crack deflectors rather than stress concentrators.

The integration of SAXS, TEM, and mechanical testing establishes quantitative structure-property relationships, validating the modified Guth-Gold model while identifying its limitations at high loadings (>45 wt.%). Aging studies further highlight the role of post-processing optimization, with *cis*-PI composites showing a 25% hardness increase after 160 hours, offering practical insights for industrial applications.

These findings challenge conventional nanocomposite design paradigms by demonstrating that optimal mechanical performance does not always require perfect dispersion, particularly in rigid matrices. The work provides a roadmap for tailoring PI-Sio_2 composites to specific applications—*cis*-PI for high-strain uses (e.g., tires) and *trans*-PI for high-strength needs (e.g., medical devices). Future research should explore surface modifications to further enhance *trans*-PI dispersion while preserving its unique strengthening mechanisms.

By unifying multiscale characterization with mechanical analysis, this study advances the scientific foundation for elastomer nanocomposites while delivering actionable strategies for material engineers. The results underscore the importance of matrix-filler interplay in designing next-generation nanocomposites with customized properties.

References

[1] Schmidt, D.; Shah, D.; Giannelis, E. P. New Advances in Polymer/Layered Silicate Nanocomposites. Curr. Opin. Solid State Mater. Sci. 2002, *6* (3), 205–212. https://doi.org/10.1016/S1359-0286(02)00049-9.

[2] Paul, D. R.; Robeson, L. M. Polymer Nanotechnology: Nanocomposites. Polymer 2008, *49* (15), 3187–3204. https://doi.org/10.1016/j.polymer.2008.04.017.

[3] Jordan, J.; Jacob, K. I.; Tannenbaum, R.; Sharaf, M. A.; Jasiuk, I. Experimental Trends in Polymer Nanocomposites—A Review. Mater. Sci. Eng. A 2005, *393* (1–2), 1–11. https://doi.org/10.1016/j.msea.2004.09.044.

[4] Bokobza, L. Multiwall Carbon Nanotube Elastomeric Composites: A Review. Polymer 2007, *48* (17), 4907–4920. https://doi.org/10.1016/j.polymer.2007.06.046.

[5] Raquez, J.-M.; Habibi, Y.; Murariu, M.; Dubois, P. Polylactide (PLA)-Based Nanocomposites. Prog. Polym. Sci. 2013, *38* (10–11), 1504–1542. https://doi.org/10.1016/j.progpolymsci.2013.05.014.

[6] Wu, H.; Wang, W.; Huang, Y.; Sui, X.; Zhou, X. Comprehensive Study on Graphene Oxide and Carbon Nanotube einforcement of Polylactide Nanocomposites: Morphology, Mechanical Properties and Durability. Ind. Eng. Chem. Res. 2019, *58* (25), 10888–10898. https://doi.org/10.1021/acs.iecr.9b00815.

[7] Treloar, L. R. G. The Physics of Rubber Elasticity, 3rd ed.; Oxford University Press: Oxford, 2005.

[8] Mark, J. E.; Erman, B.; Roland, M. The Science and Technology of Rubber, 4th ed.; Academic Press: Cambridge, 2013.

[9] Gent, A. N. Engineering with Rubber: How to Design Rubber Components, 3rd ed.; Hanser: Munich, 2012.

[10] Huneau, B. Strain-Induced Crystallization of Natural Rubber: A Review of X-Ray Diffraction Investigations. Rubber Chem. Technol. 2011, *84* (3), 425–452. https://doi.org/10.5254/1.3601131.

[11] Rault, J.; Marchal, J.; Judenstein, P.; Albouy, P. A. Stress-Induced Crystallization and Reinforcement in Filled Natural Rubbers: 2H NMR Study. Macromolecules 2006, *39* (24), 8356–8368. https://doi.org/10.1021/ma061308n.

[12] Behera, P. K.; Sahu, B.; Rautaray, D.; Pandey, K. K. Trans-Polyisoprene Based Shape Memory Polymer for Biomedical Applications. J. Mech. Behav. Biomed. Mater. 2020, *110*, 103885. https://doi.org/10.1016/j.jmbbm.2020.103885.

[13] Lendlein, A.; Kelch, S. Shape-Memory Polymers. Angew. Chem. Int. Ed. 2002, *41* (12), 2034–2057. https://doi.org/10.1002/1521-3773(20020617)41:12<2034::AID-ANIE2034>3.0.CO;2-M.

[14] Maiti, M.; Bhattacharya, M.; Bhowmick, A. K. Elastomer Nanocomposites. Rubber Chem. Technol. 2008, *81* (3), 384–469. https://doi.org/10.5254/1.3548219.

[15] Thomas, S.; Stephen, R. Rubber Nanocomposites: Preparation, Properties, and Applications; Wiley: Singapore, 2010.

[16] Karger-Kocsis, J.; Mészáros, L.; Bárány, T. Ground Tyre Rubber (GTR) in Thermoplastic Composites: A Review. J. Reinf. Plast. Compos. 2013, *32* (5), 296–308. https://doi.org/10.1177/0731684412468880.

[17] Schaefer, D. W.; Justice, R. S. How Nano Are Nanocomposites? Macromolecules 2007, *40* (24), 8501–8517. https://doi.org/10.1021/ma070356w.

[18] Sternstein, S. S.; Zhu, A.-J. Reinforcement Mechanism of Nanofilled Polymer Melts as Elucidated by Nonlinear Viscoelastic Behavior. Macromolecules 2002, *35* (19), 7262–7273. https://doi.org/10.1021/ma020482u.

[19] Starr, F. W.; Schrøder, T. B.; Glotzer, S. C. Effects of a Nanoscopic Filler on the Structure and Dynamics of a Simulated Polymer Melt and the Relationship to Ultrathin Films. Phys. Rev. E 2001, *64* (2), 021802. https://doi.org/10.1103/PhysRevE.64.021802.

[20] Guth, E. Theory of Filler Reinforcement. J. Appl. Phys. 1945, *16* (1), 20–25. https://doi.org/10.1063/1.1707495.

[21] Smallwood, H. M. Limiting Law of the Reinforcement of Rubber. J. Appl. Phys. 1944, *15* (11), 758–766. https://doi.org/10.1063/1.1707385.

[22] Huber, G.; Vilgis, T. A. On the Mechanism of Hydrodynamic Reinforcement in Elastic Composites. Macromolecules 2002, *35* (24), 9204–9210. https://doi.org/10.1021/ma020415v.

[23] Gersappe, D. Molecular Mechanisms of Failure in Polymer Nanocomposites. Phys. Rev. Lett. 2002, *89* (5), 058301. https://doi.org/10.1103/PhysRevLett.89.058301.

[24] Sternstein, S. S.; Zhu, A.-J. Reinforcement Mechanism of Nanofilled Polymer Melts as Elucidated by Nonlinear Viscoelastic Behavior. Macromolecules 2002, *35* (19), 7262–7273. https://doi.org/10.1021/ma020482u.

[25] Kumar, S. K.; Krishnamoorti, R. Nanocomposites: Structure, Phase Behavior, and Properties. Annu. Rev. Chem. Biomol. Eng. 2010, *1*, 37–58. https://doi.org/10.1146/annurev-chembioeng-073009-100856.

[26] Mackay, M. E.; Tuteja, A.; Duxbury, P. M.; Hawker, C. J.; Van Horn, B.; Guan, Z.; Chen, G.; Krishnan, R. S. General Strategies for Nanoparticle Dispersion. Science 2006, *311* (5768), 1740–1743. https://doi.org/10.1126/science.1122225.

[27] Bockstaller, M. R.; Mickiewicz, R. A.; Thomas, E. L. Block Copolymer Nanocomposites: Perspectives for Tailored Functional Materials. Adv. Mater. 2005, *17* (11), 1331–1349. https://doi.org/10.1002/adma.200500167.

[28] Ohno, K.; Morinaga, T.; Koh, K.; Tsujii, Y.; Fukuda, T. Synthesis of Monodisperse Silica Particles Coated with Well-Defined, High-Density Polymer Brushes by Surface-Initiated Atom Transfer Radical Polymerization. Macromolecules 2005, *38* (6), 2137–2142. https://doi.org/10.1021/ma048011q.

[29] Pyun, J.; Matyjaszewski, K. Synthesis of Nanocomposite Organic/Inorganic Hybrid Materials Using Controlled/"Living" Radical Polymerization. Chem. Mater. 2001, *13* (10), 3436–3448. https://doi.org/10.1021/cm0109987.

[30] Zhao, B.; Brittain, W. J. Polymer Brushes: Surface-Immobilized Macromolecules. Prog. Polym. Sci. 2000, *25* (5), 677–710. https://doi.org/10.1016/S0079-6700(00)00012-5.

[31] Rong, M. Z.; Zhang, M. Q.; Zheng, Y. X.; Zeng, H. M.; Friedrich, K. Improvement of Tensile Properties of Nano-SiO_2/PP Composites in Relation to Percolation Mechanism. Polymer 2001, *42* (7), 3301–3304. https://doi.org/10.1016/S0032-3861(00)00726-8.

[32] Zhang, Q.; Archer, L. A. Poly(ethylene oxide)/Silica Nanocomposites: Structure and Rheology. Langmuir 2002, *18* (26), 10435–10442. https://doi.org/10.1021/la026338j.

[33] Jouault, N.; Vallat, P.; Dalmas, F.; Said, S.; Jestin, J.; Boué, F. Well-Dispersed Fractal Aggregates as Filler in Polymer–Silica Nanocomposites: Long-Range Effects in Rheology. Macromolecules 2009, *42* (6), 2031–2040. https://doi.org/10.1021/ma8019084.

[34] Ajayan, P. M.; Schadler, L. S.; Braun, P. V. Nanocomposite Science and Technology; Wiley-VCH: Weinheim, 2003.

[35] Balazs, A. C.; Emrick, T.; Russell, T. P. Nanoparticle Polymer Composites: Where Two Small Worlds Meet. Science 2006, *314* (5802), 1107–1110. https://doi.org/10.1126/science.1130557.

[36] Moniruzzaman, M.; Winey, K. I. Polymer Nanocomposites Containing Carbon Nanotubes. Macromolecules 2006, *39* (16), 5194–5205. https://doi.org/10.1021/ma060733p.

[37] Jancar, J.; Douglas, J. F.; Starr, F. W.; Kumar, S. K.; Cassagnau, P.; Lesser, A. J.; Sternstein, S. S.; Buehler, M. J. Current Issues in Research on Structure–Property Relationships in Polymer Nanocomposites. Polymer 2010, *51* (15), 3321–3343. https://doi.org/10.1016/j.polymer.2010.02.044.

[38] Krishnamoorti, R.; Vaia, R. A. Polymer Nanocomposites: Synthesis, Characterization, and Modeling; ACS Symposium Series; American Chemical Society: Washington, DC, 2002.

[39] Schaefer, D. W.; Zhao, J.; Brown, J. M.; Anderson, D. P.; Tomlin, D. W. Morphology of Dispersed Carbon Single-Walled Nanotubes. Chem. Phys. Lett. 2003, *375* (3–4), 369–375. https://doi.org/10.1016/S0009-2614(03)00955-3.

[40] Sternstein, S. S.; Zhu, A.-J. Reinforcement Mechanism of Nanofilled Polymer Melts as Elucidated by Nonlinear Viscoelastic Behavior. Macromolecules 2002, *35* (19), 7262–7273. https://doi.org/10.1021/ma020482u.

[41] Gersappe, D. Molecular Mechanisms of Failure in Polymer Nanocomposites. Phys. Rev. Lett. 2002, *89* (5), 058301. https://doi.org/10.1103/PhysRevLett.89.058301.

[42] Liu, J.; Gao, Y.; Cao, D.; Zhang, L.; Guo, Z. Nanoparticle Dispersion and Aggregation in Polymer Nanocomposites: Insights from Molecular Dynamics Simulation. Langmuir 2011, *27* (12), 7926–7933. https://doi.org/10.1021/la201073m.

[43] Celina, M. C. Review of Polymer Oxidation and Its Relationship with Materials Performance and Lifetime Prediction. Polym. Degrad. Stab. 2013, *98* (12), 2419–2429. https://doi.org/10.1016/j.polymdegradstab.2013.06.024.

[44] Colin, X.; Marais, C.; Verdu, J. Kinetic Modeling of the Aging of Brittle Epoxy Networks during Postcuring. J. Appl. Polym. Sci. 2005, *96* (4), 1138–1145. https://doi.org/10.1002/app.21547.

[45] Gillen, K. T.; Bernstein, R.; Celina, M. Challenges of Accelerated Aging Techniques for Elastomer Lifetime Predictions. Rubber Chem. Technol. 2015, *88* (1), 1–27. https://doi.org/10.5254/rct.15.84873.

[46] Lipatov, Y. S. Polymer Reinforcement; ChemTec Publishing: Toronto, 1995.

[47] Pukánszky, B. Influence of Interface Interaction on the Ultimate Tensile Properties of Polymer Composites. Composites 1990, *21* (3), 255–262. https://doi.org/10.1016/0010-4361(90)90240-W.

[48] Brune, D. A.; Bicerano, J. Micromechanics of Nanocomposites: Comparison of Tensile and Compressive Elastic Moduli, and Prediction of Effects of Incomplete Exfoliation and Imperfect Alignment on Modulus. Polymer 2002, *43* (2), 369–387. https://doi.org/10.1016/S0032-3861(01)00634-4.

[49] Vaia, R. A.; Giannelis, E. P. Polymer Nanocomposites: Status and Opportunities. MRS Bull. 2001, *26* (5), 394–401. https://doi.org/10.1557/mrs2001.93.

[50] Tjong, S. C. Structural and Mechanical Properties of Polymer Nanocomposites. Mater. Sci. Eng. R Rep. 2006, *53* (3–4), 73–197. https://doi.org/10.1016/j.mser.2006.06.001.

[51] Glatter, O.; Kratky, O. Small Angle X-Ray Scattering; Academic Press: London, 1982.

[52] Thomas, S.; Zaikov, G. E.; Valsaraj, S. V. Recent Advances in Polymer Nanocomposites; Brill: Leiden, 2009.

[53] Thostenson, E. T.; Li, C.; Chou, T.-W. Nanocomposites in Context. Compos. Sci. Technol. 2005, *65* (3–4), 491–516. https://doi.org/10.1016/j.compscitech.2004.11.003.

[54] Ajayan, P. M.; Schadler, L. S.; Braun, P. V. Nanocomposite Science and Technology; Wiley-VCH: Weinheim, 2003.

[55] Celina, M.; Linde, E.; Martinez, E. Carbonyl Identification and Quantification Uncertainties for Oxidative Polymer Degradation. Polym. Degrad. Stab. 2021, *188*, 109550. https://doi.org/10.1016/j.polymdegradstab.2021.109550.

[56] Gillen, K. T.; Bernstein, R.; Derzon, D. K. Evidence of Non-Arrhenius Behaviour from Laboratory Aging and 24-Year Field Aging of Polychloroprene Rubber Materials. Polym. Degrad. Stab. 2005, *87* (1), 57–67. https://doi.org/10.1016/j.polymdegradstab.2004.07.008.

[57] Koo, J. H. Polymer Nanocomposites: Processing, Characterization, and Applications; McGraw-Hill: New York, 2006.

[58] Utracki, L. A. Clay-Containing Polymeric Nanocomposites; Rapra Technology: Shawbury, 2004.